Comparison of Technetium-99m Pyrophosphate and Technetium-99m DTPA Aerosols for SPECT Ventilation Lung Imaging

Ali T. Isitman, B. David Collier, David W. Palmer, LisaAnn Trembath, Arthur Z. Krasnow, Shyam A. Rao, Robert S. Hellman, Raymond G. Hoffmann, David C. Peck, and Charles J. Dellis

Department of Radiology, Department of Biostatistics, Medical College of Wisconsin, Milwaukee, Wisconsin

Although [^{99m}Tc] diethylenetriaminepentaacetic acid (DTPA) is currently the most widely used radioaerosol, rapid alveolar clearance limits its usefulness for single photon emission computed tomography (SPECT) ventilation lung imaging. Previous research has shown that [^{99m}Tc]phosphate compounds have high alveolar deposition and slow clearance and thus provide suitable aerosols for pulmonary ventilation studies. We have compared the pulmonary retention and blood levels of [^{99m}Tc]pyrophosphate (PYP) and [^{99m}Tc]DTPA in eight normal nonsmoking male volunteers. These two radioaerosols have comparable pulmonary deposition. Technetium-99m PYP, however, has a much slower pulmonary clearance which allows sufficient time (20 or more minutes) for SPECT data acquisition using a single-headed rotating gamma camera. While the radiation absorbed dose to the lungs for [^{99m}Tc]PYP (0.31 rad/mCi) is greater than for [^{99m}Tc]DTPA (0.11 rad/mCi), it is at a clinically acceptable and safe level.

J Nucl Med 29:1761–1767, 1988

Single photon emission computed tomography (SPECT) imaging of lung perfusion using technetium-99m macroaggregated albumin ([^{99m}Tc]MAA) has been shown to increase the sensitivity and specificity with which pulmonary emboli are detected (*1–5*). Performing SPECT ventilation lung imaging, however, is more difficult because of the lack of a suitable radioaerosol. Characteristics of the ideal radioaerosol for SPECT ventilation lung imaging should include minimal major airway adherence, high alveolar deposition, low transalveolar absorption, slow clearance from the lungs (to satisfy the 20 min or more required for SPECT data acquisition), and acceptable radiation absorbed dose. When used before perfusion lung imaging, technetium-99m diethylenetriaminepentaacetic acid ([^{99m}Tc] DTPA) aerosol can provide planar ventilation lung images of acceptable diagnostic quality (*6–9*). It has been demonstrated, however, that [^{99m}Tc]DTPA has a relatively rapid clearance from the alveoli which increases further in various pulmonary diseases (*9*). This rapid alveolar clearance which results in low peripheral count rate limits the usefulness of this radioaerosol for SPECT ventilation lung imaging (*10–11*).

We previously reported that several ^{99m}Tc-labeled phosphate compounds (hexophosphate inositol and diphosphonate) have a low clearance rate from the lungs (*12–15*). In this study, we have investigated the feasibility of using [^{99m}Tc]pyrophosphate ([^{99m}Tc]PYP), a chemically similar compound which is widely available for human use, as a radioaerosol for SPECT ventilation lung imaging.

MATERIALS AND METHODS

To investigate the potential of [^{99m}Tc]PYP and [^{99m}Tc] DTPA aerosols for SPECT ventilation lung imaging, eight normal nonsmoking male volunteers were studied with both radioaerosols. These subjects ranged in age from 20 to 40 yr (mean 26 yr), were in good health, and had no history of cardiac or pulmonary disease. Each subject gave informed consent to participate in this protocol which was approved and monitored by an Institutional Review Committee. Each subject participated in two radioaerosol studies, one with each

Received Sept. 29, 1987; revision accepted June 27, 1988.

For reprints contact: Ali T. Isitman, MD, Nuclear Medicine Division, Milwaukee Co. Medical Complex, 8700 W. Wisconsin Ave., Milwaukee, WI 53226.

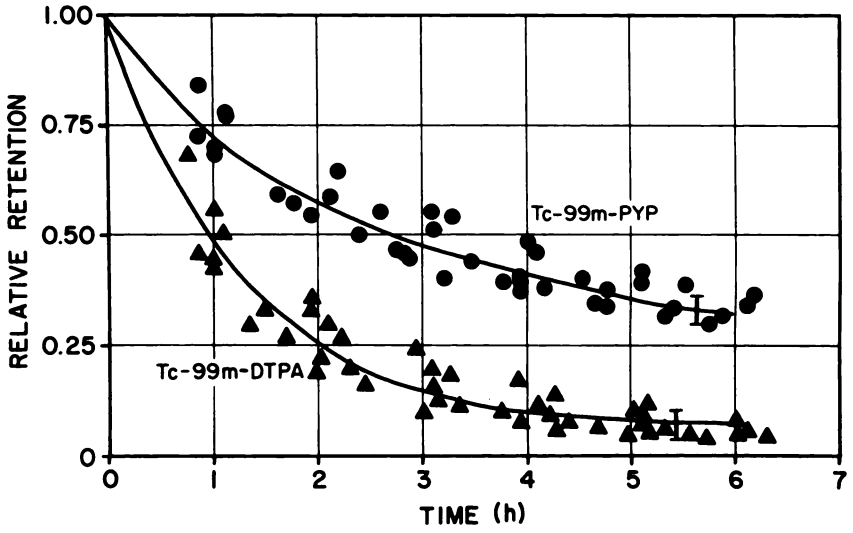

FIGURE 1
Time variation of the normalized pulmonary count rates for [^{99m}Tc]PYP and [^{99m}Tc]DTPA aerosols following inhalation. Data points represent eight normal nonsmoking volunteers. Solid lines are least squares fits using the formula $(Ae^{Bt} + C)e^{-0.115t}$, where t is the time in hours, constrained to one at t = 0. For PYP: A = 0.372, B = -0.664 hr^{-1}, and C = 0.628. For DTPA: A = 0.883, B = -0.722 hr^{-1}, and C = 0.117. For the fits, representative 99% confidence limits are shown by the vertical bars near 5.5 hr.

of the agents (PYP or DTPA). The two sequential studies were performed at least one and no more than 16 wk apart. Vital signs were monitored, and any complications such as pulmonary distress were noted. In addition, volunteers were contacted 1 wk after participating in the study and asked about late or delayed side effects.

Commercially available DTPA kits (Medi-Physics, Inc., Richmond, CA) were used to prepare [^{99m}Tc]DTPA in accordance with the manufacturer's recommendations. Technetium-99m PYP was prepared using a modified version of the method of Huberty et al. (*16*). Huberty's final pH values were between 3.0 and 3.5, while our modified method produced a final pH of 5.2 to 5.5. Commercially available nebulizers (UltraVent Radioaerosol Delivery System, Mallinckrodt, Inc., St. Louis, MO and Lung Aerosol Unit, Cadema Medical Products, Inc., Middletown, NY) were used to administer the two agents as aerosols. Thirty millicuries of the chosen agent ([^{99m}Tc]PYP or [^{99m}Tc]DTPA) in ~3 ml was placed in the nebulizer, and inhalation was performed for 5 min of normal tidal breathing with 13 l/min of oxygen flowing through the nebulizer.

To assess the distribution of activity in the lungs, images from six views were acquired at zero and 3 hr following inhalation of the radioaerosol using a gamma camera interfaced to a computer (low-energy general purpose collimator, 20% window, 500,000 counts for each view). Posterior view images were acquired hourly to observe temporal behavior of the distribution and to provide data needed for calculation of the radiation absorbed dose to the lungs. Required for the dose calculation (discussed further below) is the lung-region activity at various times postinhalation, AL(t). This is easily shown to equal RL(t)/C, where RL(t) is the background corrected count rate (obtained from a region of interest (ROI) drawn around the lungs on the posterior digital images taken at time (t), and C is the count rate per mCi in the lungs. An average value of the factor C was determined by imaging in the manner described above two male volunteers following injection of a known activity of [^{99m}Tc]MAA. Under the assumption that all injected activity is trapped in the lungs, the lung-ROI count rates from the [^{99m}Tc]MAA studies permitted calculation of C.

To obtain the activity (mCi) in the blood at various times after inhalation of the radioaerosol, AB(t), 1 ml venous blood samples were drawn at times t = 0, 5, 10, 15, 20, 40, and 60 min. At T hours postinhalation (~24 hr), their average count rate RB(t), was determined (in duplicate, using a gamma well counter), then corrected for decay in the time interval between counting and collection, (T-t), and multiplied by the subject's

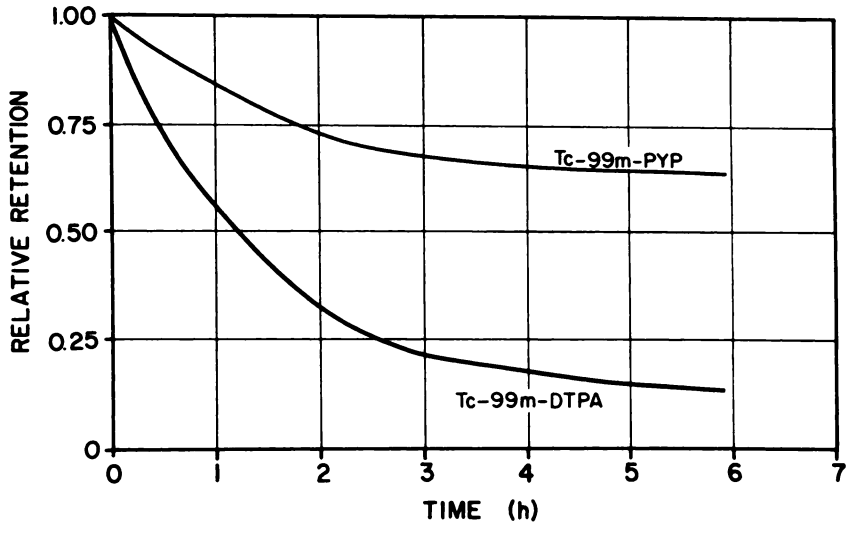

FIGURE 2
Time variation of the normalized and decay corrected nonlinear, least squares fits to the pulmonary count rate data (see Fig. 1) for [^{99m}Tc]PYP and [^{99m}Tc]DTPA aerosols following inhalation. Note the prolonged pulmonary retention of PYP.

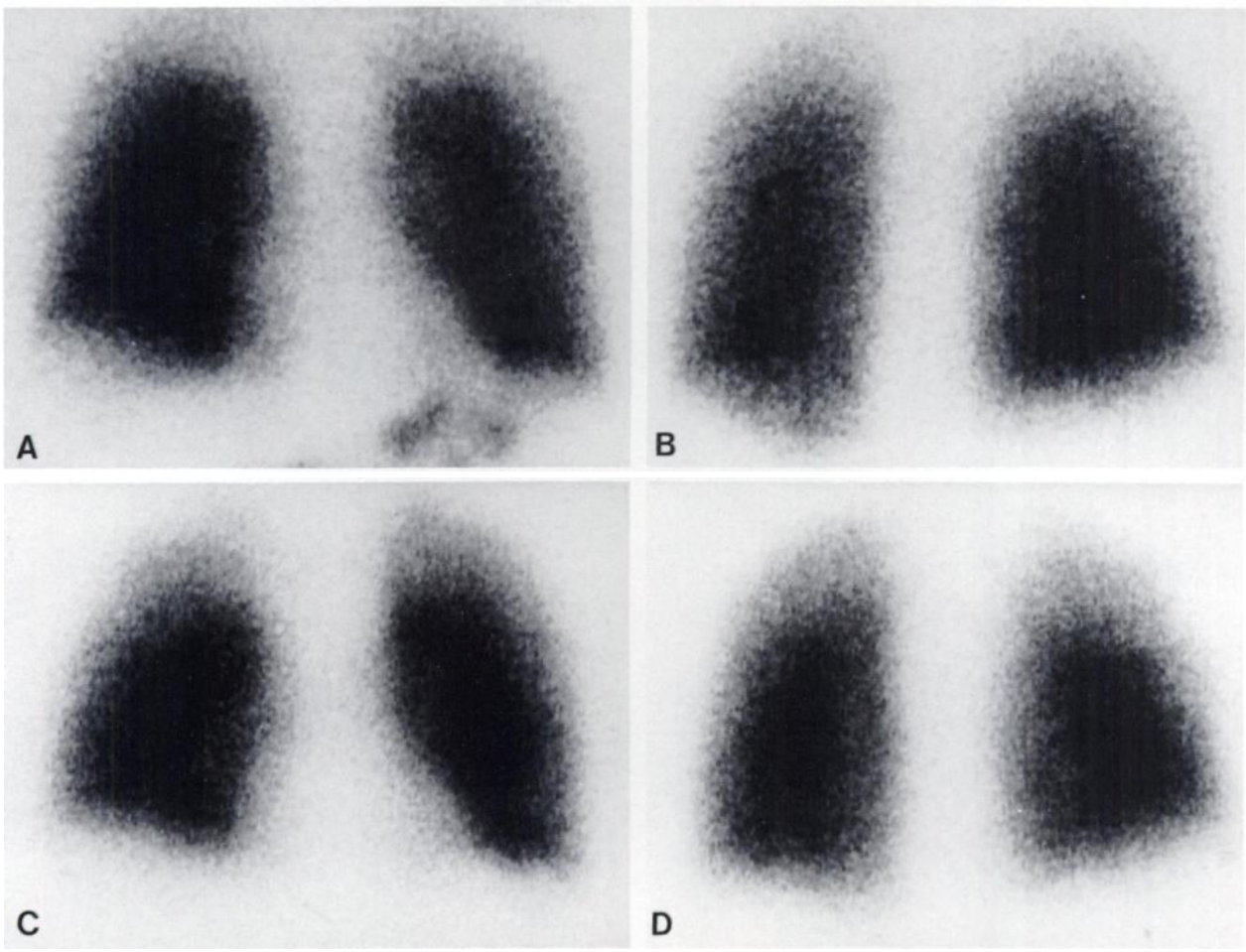

FIGURE 3
Anterior [^{99m}Tc]PYP (A), posterior [^{99m}Tc]PYP (B), anterior [^{99m}Tc]MAA (C), and posterior [^{99m}Tc]MAA (D) planar images. Note the similarity in pulmonary distribution and imaging characteristics for these supine radioaerosol ventilation and perfusion images obtained 1 wk apart in the same normal volunteer. Also note the absence of bony uptake of [^{99m}Tc]PYP due to the low transalveolar absorption of this radioaerosol.

total blood volume, V (determined from a height-and-weight nomogram) to give the total blood count rate at time t. Finally, the result was divided by the well counter sensitivity S, CPM/mCi (determined by counting samples of known activity) to yield the value AB(t).

Nonlinear least squares fits were made to all lung field activity data, AL(t), from which was calculated the average cumulated activity (area under the curve out to infinity) for both agents. These values were then used to determine the radiation absorbed dose to the lungs following the MIRD methodology (*17–18*).

In six other volunteers (normal and abnormal), SPECT studies were acquired using a 500-mm rotating gamma camera fitted with a low-energy, general purpose collimator. SPECT data was acquired for 64 views (20 sec/view, 128 × 128 matrix) over 360° of circular gamma camera rotation. Following uniformity correction and filtering (pre-processing Hanning filter with a frequency cutoff of 0.8 cycles/cm), transaxial images were reconstructed using filtered backprojection with a ramp filter. Coronal, sagittal, and transaxial SPECT images were displayed as three pixel (1.2 cm) thick tomographic sections.

After the pattern of [^{99m}Tc]PYP aerosol studies was established in normal lungs, 29 patients were examined by this technique. They were referred for regional quantitation of pulmonary function (n=10), evaluation of pulmonary embolism (n=15) and other diagnoses (n=4).

RESULTS

Regions of interest drawn around the posteriorly viewed lungs in the [^{99m}Tc]MAA studies on two volunteers yielded C = 152,000 cts/min/mCi of ^{99m}Tc in the lungs, differing by <0.5% between the two. Regions drawn on the posteriorly viewed lungs immediately postinhalation for [^{99m}Tc]PYP and[^{99m}Tc]DTPA yielded eight-subject mean count rates of 150,200 and 152,100 CPM, respectively, with a standard deviation of ~55%. Hence, when multiplied by C, 5 min of normal tidal breathing of either of the agents is found to deposit almost exactly 1 mCi in the lungs.

In like manner, lung-field ROI count rates taken from the hourly posterior view images permit determi-

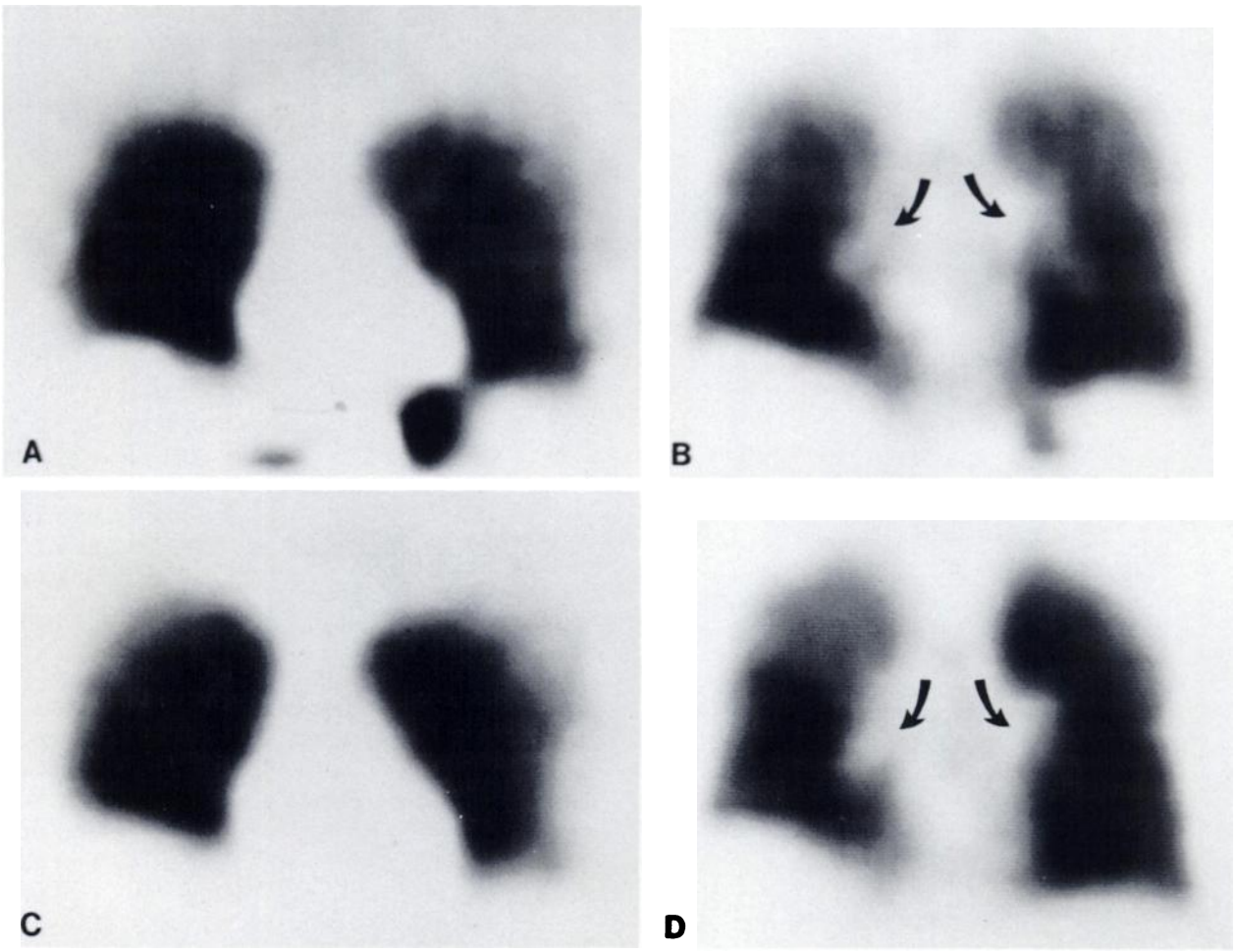

FIGURE 4
Selected coronal [^{99m}Tc]PYP aerosol ventilation (A and B) and [^{99m}Tc]MAA perfusion (C and D) SPECT images obtained at the same times as the planar images in Figure 3. The cardiac and mediastinal silhouette is well defined. Hilar structures which are indistinct on the planar images are well delineated (arrows).

nation of the normalized pulmonary activity, AL(t)/AL(0), over 6 hr. Figure 1 shows the pulmonary activity measured from the eight subjects (data points) and the nonlinear least squares fits (solid lines). Clearly, there is significantly longer pulmonary retention of [^{99m}Tc]PYP than of [^{99m}Tc]DTPA, their respective 50% retention times being 2.8 and 0.9 hr on the fitted curves. When these curves are decay corrected (Fig. 2), they show that 64% of PYP and 13% of DTPA remained in the lungs 6 hr after inhalation.

Activity in the blood at 30 min following inhalation, relative to the initially deposited activity, i.e., AB(30)/AL(0), was 3.3% for [^{99m}Tc]PYP and 6.8% for [^{99m}Tc]DTPA. At 60 min the respective values were 3.9% and 7.6%.

Integration of the fitted lung field time-activity curves out to infinity yields cumulated activities of 5.94 mCi-hr for [^{99m}Tc]PYP and 2.07 mCi-hr for [^{99m}Tc]DTPA for each mCi deposited. This activity is assumed to be in the lungs. When multiplied by the absorbed dose per unit cumulated activity, obtained from standard tabulations (*17*), the absorbed dose to the lungs is found to be 0.31 and 0.11 rad/mCi initially deposited in the lungs, respectively, for [^{99m}Tc]PYP and [^{99m}Tc]DTPA.

Inhalation of [^{99m}Tc]DTPA or [^{99m}Tc]PYP aerosols caused no side effects. Both radiopharmaceuticals showed no significant adherence in the major airways of normal volunteers and produced good quality immediate postinhalation planar images. However, count rates dropped significantly during the acquisition of a six-view planar ventilation study using [^{99m}Tc]DTPA, thus requiring prolonged time periods to collect 500,000 counts in the later views. In contrast, satisfactory six-view planar ventilation images were obtained using [^{99m}Tc]PYP aerosol even 3 hr after inhalation. It was possible to perform both pre-perfusion and postperfusion SPECT ventilation imaging with this agent. Figure 3 shows 500,000 count planar [^{99m}Tc]PYP ventilation images in a normal volunteer which have been matched with 500,000 count [^{99m}Tc]MAA images obtained 1 wk later. The similarity in alveolar distribution and imaging characteristics for these supine ^{99m}Tc ventilation

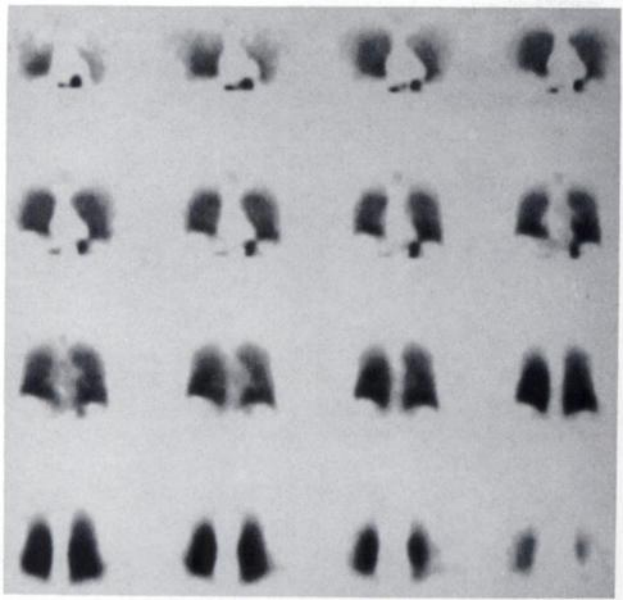

FIGURE 5
Complete set of anterior to posterior sequential 1.2-cm-thick coronal [^{99m}Tc]PYP aerosol SPECT images in a normal nonsmoking volunteer.

and perfusion studies is striking. Given the normal physiologic match between pulmonary ventilation and perfusion, this result is to be expected. Figure 4 shows selected coronal [^{99m}Tc]PYP and [^{99m}Tc]MAA SPECT images obtained in the same normal volunteer as shown in Figure 3. The cardiac-and-mediastinal silhouette is well defined. In addition, hilar structures which are indistinct on the planar images can easily be delineated. A complete set of coronal [^{99m}Tc]PYP aerosol SPECT ventilation images for this normal subject is shown in Figure 5. Figure 6 shows the images of a patient with chronic obstructive lung disease referred for evaluation of pulmonary embolism. On comparing the immediate postperfusion [^{99m}Tc]PYP SPECT ventilation images with the SPECT perfusion images, besides showing matching defects, two large areas of ventilation/perfusion mismatch suspicious for pulmonary embolism became evident.

DISCUSSION

SPECT, which provides improved contrast resolution and more complete three-dimensional spatial information than can be achieved with planar imaging, has been successfully applied to a number of common nuclear medicine examinations including [^{99m}Tc]MAA perfusion lung imaging (*1–5,19*). Application of SPECT to ventilation lung imaging, however, has been limited by the requirement that the distribution of radioaerosol within the lungs remain relatively stable during the 20 min or more typically required for SPECT data acquisition with a single-headed rotating gamma camera. If the distribution of radioaerosol were to change significantly during the time of SPECT data acquisition, unacceptable incomplete angular sampling artifacts might be created. Thus, while [^{99m}Tc]DTPA has a clearance rate that does not usually interfere significantly with pre-perfusion planar ventilation imaging, this radioaerosol clears too rapidly for optimal SPECT imaging (*10*). Previously investigated radioaerosols with alveolar clearance rates lower than [^{99m}Tc]DTPA include [^{99m}Tc]sulfur colloid and [^{99m}Tc]human serum albumin. Unfortunately both of these agents, when inhaled, tend to deposit in major airways as well as in alveoli (*20–23*). Nitrogen-13 (for PET) and Krypton-81m (for SPECT) gases have been successfully used for tomographic ventilation lung imaging (*10,24,25*). However, neither of these techniques has been widely adopted, perhaps due to the cost and the limited availability of these agents. Therefore, in searching for a radiopharmaceutical potentially appropriate for SPECT ventilation lung imaging at a wide range of nuclear medicine facilities, a [^{99m}Tc]phosphate compound was investigated. Previous research, using only planar imaging showed that both hexophosphate inositol and diphosphonate have high alveolar deposition and prolonged retention (*12–15*), which suggests that these agents might be suitable for SPECT imaging. However, in many countries including the United States hexophosphate inositol and diphosphonate are not commercially available for human use. Therefore, we chose to explore the potential usefulness of the chemically related and more widely available [^{99m}Tc]PYP as a radiopharmaceutical for SPECT ventilation lung imaging.

Results reported in this article show that [^{99m}Tc]PYP has a high alveolar deposition, comparable to that of [^{99m}Tc]DTPA. In addition, the relatively slow pulmonary clearance of [^{99m}Tc]PYP easily permits more than enough time and counts for SPECT data acquisition. In most clinical settings, SPECT ventilation lung imaging is begun immediately following inhalation so as to take advantage of the high count rate at that time. Our preliminary results on clinically referred patients, all of whom were successfully imaged with this technique, are encouraging. Given that the technical feasibility of high quality [^{99m}Tc]PYP SPECT ventilation lung imaging has been demonstrated (Figs. 4–6), further clinical research is needed to establish the diagnostic efficacy of this technique for various lung disorders. Furthermore, unlike [^{99m}Tc]DTPA, the stable alveolar distribution of [^{99m}Tc]PYP permits postperfusion planar ventilation lung imaging where a comparably high count rate from the radioaerosol is needed to

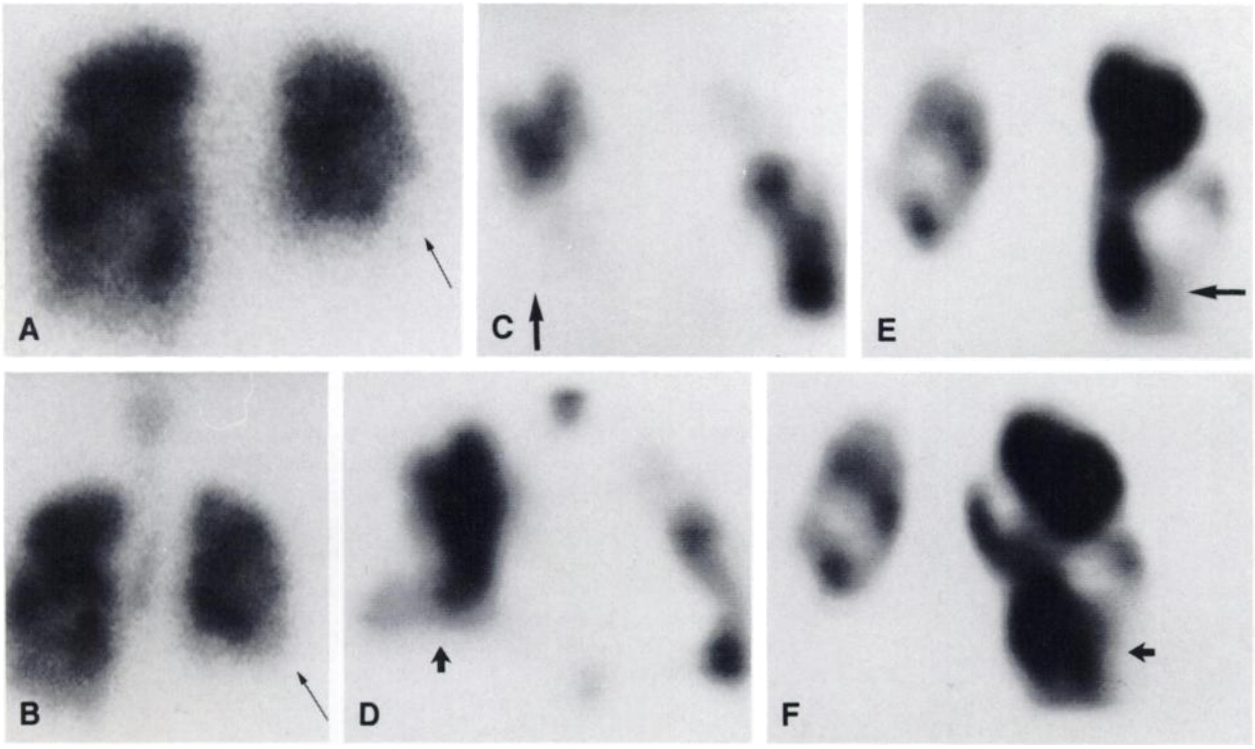

FIGURE 6
Adult patient with chronic obstructive lung disease suspected of having pulmonary embolism. Posterior [^{99m}Tc]MAA (A) and immediate postperfusion [^{99m}Tc]PYP (B) planar images show matching defects and a ventilation/perfusion mismatch in the right lower lung field (long arrows). Selected coronal [^{99m}Tc]MAA SPECT images (C and D) and corresponding [^{99m}Tc]PYP SPECT images (E and F) show ventilation/perfusion mismatches in both lower lung fields (long and short arrows).

match or overcome the persisting activity from residual [^{99m}Tc]MAA. It is tempting to speculate that the high alveolar deposition and retention of PYP might also provide a vehicle for delivery of therapeutic agents. While the mechanism of alveolar uptake and retention of [^{99m}Tc]phosphates is not completely understood, there is evidence that phosphate receptors on the alveolar membrane may play an important role. These compounds may chemically incorporate into surfactant or bind to available alveolar phosphate receptors with their free phosphate radicals (*12–15*).

We conclude that when compared to [^{99m}Tc]DTPA and other ^{99m}Tc radiopharmaceuticals which have been used for aerosol ventilation lung imaging, [^{99m}Tc]PYP has the desirable properties for SPECT imaging of low major airway adherence, high pulmonary deposition and retention, and slow transalveolar absorption. In this paper, the estimated radiation absorbed dose to the lungs for [^{99m}Tc]PYP aerosol was calculated with the simplifying assumptions that (a) counts from a pulmonary ROI can be treated as activity in the lungs and (b) organs outside of the pulmonary ROI contributed a negligible amount to the lung dose. A complete and correct dosimetry for [^{99m}Tc]PYP aerosol requires measurement of biodistribution over time in multiple organs and remains a topic for future research. However, since <10% of the radioaerosol initially deposited in the lungs ever becomes blood borne, it is clear that the true radiation absorbed dose to the lungs can differ very little from the results reported here. Based on these assumptions, the estimated radiation absorbed dose to the lung for [^{99m}Tc]PYP (0.33 rad/mCi) is three times greater than for [^{99m}Tc]DTPA (0.10 rad/mCi). However, it is only moderately higher than the lung radiation absorbed dose of [^{99m}Tc]MAA (0.22 rad/mCi) (*18*) on a per millicurie basis. Since ~1 mCi of [^{99m}Tc]PYP aerosol is deposited using the proposed protocol, the radiation absorbed dose to the lungs is at a clinically acceptable and safe level. Further clinical investigation of the diagnostic efficacy of SPECT and planar postperfusion [^{99m}Tc]PYP ventilation lung imaging appears warranted.

ACKNOWLEDGMENTS

This work was supported by the General Clinical Research Center Grant No. RR00058.

The secretarial assistance of Margaret Steinmetz is greatly appreciated.

REFERENCES

1. Khan BO, Ell PJ, Jarritt PH, et al. Radionuclide section scanning of the lungs in pulmonary embolism. *Br J Radiol* 1981; 54:586–591.
2. Donaldson RM, Kahn MJ, Raphael MJ, et al. Emission tomography in embolic lung disease: angiographic correlations. *Clin Radiol* 1982; 33:389–393.
3. Osborne DR, Jaszczak RJ, Greer K, et al. Detection of pulmonary emboli in dogs: comparison of single photon emission computed tomography, gamma camera imaging, and angiography. *Radiology* 1983; 146:493–497.
4. Osborne DR, Jaszczak R, Coleman RE. Single photon emission computed tomography and its application in the lung. *Radiol Clin N Am* 1983; 21:789–800.
5. Touya JJ, Corbus HF, Savala KM, et al. Single photon emission computed tomography in the diagnosis of pulmonary thromboembolism. *Semin Nucl Med* 1986; 16:306–336.
6. Taplin GV, Chopra SK. Lung perfusion-inhalation scintigraphy in obstructive airway disease and pulmonary embolism. *Radiol Clin N Am* 1978; 16:491–513.
7. Alderson PO, Biello DR, Gottschalk A, et al. Tc-99m-DTPA aerosol and radioactive gases compared as adjuncts to perfusion scintigraphy in patients with suspected pulmonary embolism. *Radiology* 1984; 153:516–521.
8. Smart RC, Lyons NR, Burke JJ, Wood CF. A combined procedure for 99mTc aerosol ventilation and perfusion imaging. *Eur J Nucl Med* 1985; 11:65–68.
9. Coates G, O'Brodovich H. Measurement of pulmonary epithelial permeability with 99mTc-DTPA aerosol. *Semin Nucl Med* 1986; 16:275–284.
10. Binkert BL, Esser PD, Rosen JM, et al. Methods for SPECT Tc-99m DTPA aerosol and krypton-81m ventilation imaging [Abstract]. *Radiology* 1985, 157:333.
11. Smye SW, Unsworth J. The use of single photon emission computed tomography in lung imaging with aerosols. *Nucl Med Commun* 1985; 6:397–404.
12. Isitman AT, Manoli R, Schmidt GH, Holmes RA. An assessment of alveolar deposition and pulmonary clearance of radiopharmaceuticals after nebulization. *Am J Roentgenol,* 1974; 120:776–781.
13. Holmes RA, Manoli R, Isitman AT. New radioaerosols in the study of pulmonary diseases. Proceedings of the 6th International Symposium on Nuclear Medicine. Karlovy Vary, Czechoslovakia, 1975:107–119.
14. Holmes RA, Isitman AT, Manoli R, Zimmer AM. The mechanism of pulmonary clearance of ^{99m}Tc stannous phytate [Abstract]. *Clin Res* 1974; 22:506A.
15. Isitman AT, Telatar M, Akin A, et al. Clinical significance of nebulized ^{99m}Tc-Sn-Phytate inhalation lung imaging. *J Ankara Med School* 1982; 4:9–20.
16. Huberty JP, Hattner RS, Powell MR. ^{99m}Tc pyrophosphate kit: a convenient economical and high quality skeletal imaging agent. *J Nucl Med* 1974; 15:124–126.
17. Loevinger R, Berman M. A revised schema for calculating the absorbed dose from biologically distributed radionuclides. MIRD Pamphlet No. I, Revised. New York: Society of Nuclear Medicine, 1976.
18. Snyder WS, Ford MR, Warner GG, et al. "S" absorbed dose per unit cumulated activity for selected radionuclides and organs. MIRD Pamphlet No. II. New York: Society of Nuclear Medicine, 1975.
19. Hellman RS, Collier BD. Single photon emission computed tomography: a clinical experience. In: Freeman LM, Weissmann HS, eds. *Nuclear medicine annual 1987.* New York: Raven Press, 1987:51–101.
20. Taplin GV, Poe ND, Greenberg A. Lung scanning following radioaerosol inhalation. *J Nucl Med* 1966; 7:77–87.
21. Logus JW, Jette DC, Mau SF. An improved method of sulfur colloid radioaerosol inhalation. *J Nucl Med Technol* 1983; 11:137–139.
22. Logus JW, Trajan M, Hooper HR, et al. Single photon emission computed tomography of lungs imaged with 99mTc-labeled aerosol. *J Can Assoc Radiol* 1984; 35:133–138.
23. Hayes M, Taplin GV, Sawtantra K, et al. Improved radioaerosol administration system for routine inhalation lung imaging. *Radiology* 1979; 131:256–258.
24. Murata K, Harumi I, Senda M, et al. Ventilation imaging with positron emission tomography and nitrogen 13. *Radiology* 1986; 158:303–307.
25. Lavender JP, Al-Nahhas AM, Myers MJ. Ventilation perfusion ratios of the normal supine lung using emission tomography. *Br J Radiol* 1984; 57:141–146.